

HAATI survivors replace canonical telomeres with blocks of generic heterochromatin

Devanshi Jain¹, Anna K. Hebden², Toru M. Nakamura³, Kyle M. Miller⁴ & Julia Promisel Cooper¹

The notion that telomeres are essential for chromosome linearity stems from the existence of two chief dangers: inappropriate DNA damage response (DDR) reactions that mistake natural chromosome ends for double-strand DNA breaks (DSBs), and the progressive loss of DNA from chromosomal termini due to the end replication problem. Telomeres avert the former peril by binding sequence-specific end-protection factors that control the access of DDR activities^{1,2}. The latter threat is tackled by recruiting telomerase, a reverse transcriptase that uses an integral RNA subunit to template the addition of telomere repeats to chromosome ends³. Here we describe an alternative mode of linear chromosome maintenance in which canonical telomeres are superseded by blocks of heterochromatin. We show that in the absence of telomerase, *Schizosaccharomyces pombe* cells can survive telomere sequence loss by continually amplifying and rearranging heterochromatic sequences. Because the heterochromatin assembly machinery is required for this survival mode, we have termed it 'HAATI' (heterochromatin amplification-mediated and telomerase-independent). HAATI uses the canonical end-protection protein Pot1 (ref. 4) and its interacting partner Ccq1 (ref. 5) to preserve chromosome linearity. The data suggest a model in which Ccq1 is recruited by the amplified heterochromatin and provides an anchor for Pot1, which accomplishes its end-protection function in the absence of its cognate DNA-binding sequence. HAATI resembles the chromosome end-maintenance strategy found in *Drosophila melanogaster*, which lacks specific telomere sequences but nonetheless assembles terminal heterochromatin structures that recruit end-protection factors. These findings reveal a previously unrecognized mode by which cancer cells might escape the requirement for telomerase activation, and offer a tool for studying genomes that sustain unusually high levels of heterochromatinization.

Ten to fifteen percent of cancer cells achieve unlimited proliferative potential without telomerase by using one or more method(s) termed alternative lengthening of telomeres (ALT). The modus operandi of ALT seems to involve recombination between residual telomere sequences⁶. Budding yeast survive without telomerase using a similar constellation of strategies in which either the telomeric repeats or subtelomeric elements terminating in short terminal telomere repeat tracts are repeatedly replenished by recombinational mechanisms^{7–9}. Curiously, in the absence of the nuclease ExoI, budding yeast can also maintain linear chromosomes lacking telomere sequences by forming palindromes at chromosome termini¹⁰.

Fission yeast normally use classical telomere structures for chromosome end protection. The double- and single-stranded telomeric regions are bound by a group of proteins resembling human shelterin, including the double-strand telomere binding protein Taz1 (orthologue of human TRF1 and TRF2, also known as TERF1 and TERF2), the single-strand telomere binding protein Pot1, and additional proteins

linking the single-stranded and double-stranded binding complexes^{4,5,11}. Fission yeast can survive the absence of telomerase via an unusual mechanism made possible by their low chromosome number (three per haploid genome): as telomeres are lost, ensuing chromosome end-fusion reactions join the opposing ends of each single chromosome in a cell without forming inter-chromosomal fusions^{12,13}. This yields cells harbouring three circular chromosomes that lack telomere repeats, referred to as 'circular survivors'. Fission yeast can also survive the absence of telomerase by recombining persisting telomere sequences, forming so-called 'linear survivors'¹².

While investigating differences between linear and circular telomerase-minus survivors, we deleted the *trt1*⁺ gene (which encodes the catalytic reverse transcriptase subunit of telomerase), isolated survivors and analysed their sensitivities to DSB-inducing agents. Whereas linear survivors display little or no sensitivity to these agents, circular survivors are exquisitely sensitive, with a susceptibility exceeding that of cells lacking the Rad3/ATR checkpoint regulator (Fig. 1a). Notably, a subset of *trt1Δ* survivors had an intermediate level of sensitivity; we named these HAATI survivors (Fig. 1a). Like circular survivors, HAATI cells are often elongated and have DAPI (4',6-diamidino-2-phenylindole) staining patterns indicative of compromised chromosome segregation¹² (Supplementary Fig. 2). HAATI arise very infrequently when *trt1Δ* cells are propagated by repeatedly streaking single colonies on plates, a condition under which ~95% of survivors are circular. However, as HAATI survivors have a shorter doubling time than circulars, they have a competitive advantage and are enriched when *trt1Δ* cultures are grown in liquid media (Supplementary Table 1).

To determine whether the DSB resistance of HAATI survivors stems from chromosome linearity, we investigated their chromosome structure by pulsed-field gel electrophoresis (PFGE). Chromosomes of wild-type cells or linear survivors are readily resolved by PFGE, but circular chromosomes fail to enter the gel¹² (Fig. 1b). HAATI chromosomes fail to enter gels, mirroring the behaviour of circular chromosomes (Fig. 1b). To further analyse the HAATI genome, we digested it with NotI, a rare-cutting restriction enzyme that releases twelve internal and four terminal fragments from chromosomes (Chr I and II (Chr III lacks NotI recognition sites). Ethidium bromide staining shows that the internal NotI fragments of HAATI chromosomes migrate as distinct bands whereas the terminal fragments are absent (Fig. 1d), again mirroring the behaviour of DNA from circular strains. However, Southern blot analysis reveals significant deviations from circular chromosomes. In NotI digests of circular chromosomes, the terminal fragments L, I, M and C are replaced by bands representing fused terminal fragments (L+I and C+M)¹² (Fig. 1c). These bands are absent from blots of HAATI DNA, in which the majority of hybridization signal remains in the well (Fig. 1d). PCR confirmed that the loss of L, I, M and C hybridization is not due to loss of the

¹Cancer Research UK, London Research Institute, 44 Lincoln's Inn Fields, London WC2A 3PX, UK. ²Imperial College London Ovarian Cancer Action Group, London W12 0NN, UK. ³Department of Biochemistry and Molecular Genetics, University of Illinois, Chicago, Illinois 60607, USA. ⁴Gurdon Institute, Cambridge CB2 1QN, UK.

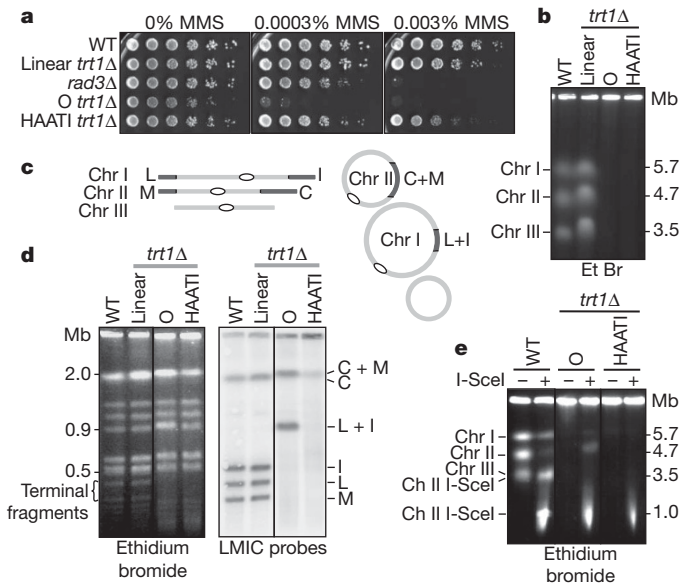


Figure 1 | Characterization of HAATI strains. **a**, HAATI are DSB resistant compared to circulars. Fivefold serial dilutions of cultures (10^7 cells ml^{-1}) were grown at 32 °C for 2 days. 'O' denotes circular. MMS, methyl methanesulphonate. **b**, HAATI whole chromosomes fail to enter pulsed-field gels. **c**, NotI digestion releases four terminal fragments, referred to as L, M, I and C, from the ends of Chr I and II; these are replaced by fusion fragments L+I and C+M in circulars. **d**, Terminal, but not internal, fragments of HAATI chromosomes fail to enter gels. Left, ethidium bromide staining of NotI digest PFG. Right, Southern blotting of PFG. **e**, Cleavage at a single I-SceI site on Chr II fails to confer gel entry to HAATI chromosomes (see also Supplementary Fig. 3). All analyses in Fig. 1 were performed on both HAATI^{rDNA} and HAATI^{STE} (see below) with identical results.

probed sequences from the genome (data not shown). Thus, HAATI chromosomes fail to exhibit the fusion fragments diagnostic of circular strains. We further reasoned that if HAATI chromosomes were circular, they would be linearized by a single chromosome cleavage, allowing entry into a gel. In contrast, if they harboured an alternative structure that prevented gel entry, for example, persistent unresolved recombination intermediates, cleavage might not lead to gel entry. To test this, we engineered a unique I-SceI site in Chr II of both HAATI and circular strains. As expected, I-SceI digestion of DNA from the engineered circular strain linearizes Chr II and confers its PFG entry (Fig. 1e and Supplementary Fig. 3). However, I-SceI digestion of the HAATI chromosome fails to confer gel entry (Fig. 1e). Similarly, the limited chromosome breakage induced by treatment with low-dose ionizing radiation fails to confer gel entry to HAATI chromosomes, whereas it does confer entry to Chr I and II of circular survivors (Supplementary Fig. 4). The inability to confer PFG entry to Chr III indicates a shared feature between HAATI chromosomes and Chr III of circular strains (discussed in legend to Supplementary Fig. 1). Thus, HAATI chromosomes are distinct from those of both linear and circular strains, most likely retaining linearity but sustaining a persistent secondary structure that prevents terminal fragments from migrating into gels.

If HAATI chromosomes are not circular, they must have ends. In considering this 'endedness', we reintroduced telomerase into circular and HAATI survivors by expressing plasmid-borne *trt1*⁺, referred to below as the '+Trt1' situation. Reintroduced Trt1 failed to affect Chr I or II of circular strains, as these chromosomes remained unable to enter PFG, whereas Chr III acquired telomeres along with the ability to enter PFG (Fig. 2a). In marked contrast, Trt1 reintroduction conferred telomere addition and PFG entry to all three HAATI survivor chromosomes (Fig. 2b, Supplementary Fig. 5).

A striking feature of HAATI+Trt1 strains is the marked alteration in chromosome size relative to wild type (Fig. 2b). These size variations occur continually before Trt1 reintroduction in HAATI cultures,

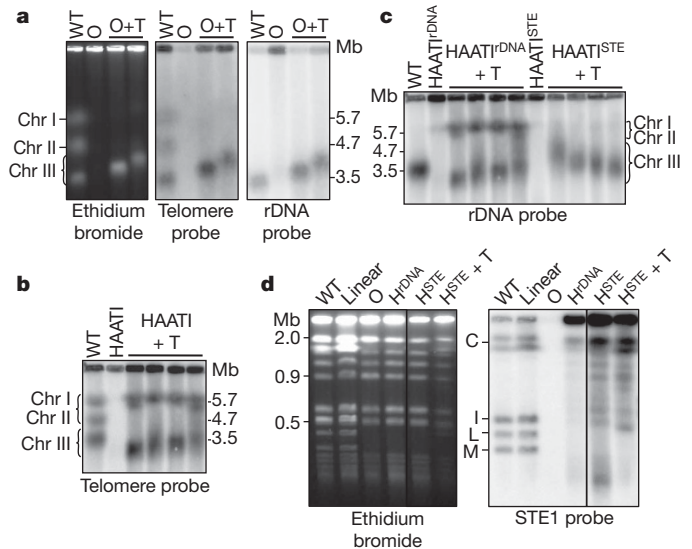


Figure 2 | Trt1 addition reveals extensive genomic rearrangements in HAATI cells. **a**, Trt1 addition to *trt1Δ* circulars results in telomere addition and gel entry of Chr III as measured by PFGE and Southern blot analysis. '+T' denotes Trt1 addition. **b**, Trt1 addition to *trt1Δ* HAATI results in telomere addition and gel entry of all three chromosomes. Cells were analysed as in **a**. **c**, rDNA has spread to all three chromosomes in HAATI^{rDNA} cells, whereas HAATI^{STE} cells contain rDNA only on Chr III (see also Supplementary Fig. 5). Cells were analysed as in **a**. **d**, NotI-digested HAATI^{STE} chromosomes have amplified STE sequences. Analysis with ('+T') and without Trt1 addition.

and chromosome sizes are stabilized once Trt1 is expressed in HAATI+Trt1 cells (Supplementary Fig. 6). Thus, HAATI *trt1Δ* survivors undergo continual and marked size alterations.

Further analysis of HAATI+Trt1 cells revealed two subsets of HAATI, hereafter referred to as HAATI^{rDNA} and HAATI^{STE}. The subtelomeric regions of wild-type Chr I and II comprise ~86 base pair imperfect repeats called sub-telomeric elements (STE), extending ~20 kilobases towards the chromosomal interior¹⁴ (Supplementary Fig. 7), whereas both telomeres of Chr III are bounded by the ribosomal DNA (rDNA) repeat regions, comprising ~10 kb repeats that span ~1 megabases¹⁵. Remarkably, while the rDNA probe hybridizes only to Chr III in wild-type cells, it hybridizes to all three chromosomes in the HAATI^{rDNA} subset (Fig. 2c), indicating that the rDNA is amplified and spread in HAATI^{rDNA} survivors. Despite the excessive levels of rDNA hybridization in HAATI^{rDNA}+Trt1 chromosomes, the rDNA probe fails to hybridize with those NotI fragments of HAATI^{rDNA} *trt1Δ* survivors that migrate upon PFGE (Supplementary Fig. 8a); this suggests that the amplified rDNA is restricted to the terminal NotI fragments that fail to enter the gels. Accordingly, on Trt1 reintroduction, the NotI fragments containing rDNA acquire the ability to enter gels (Supplementary Fig. 8a).

The HAATI^{STE} subclass of survivors exhibits a distinct pattern of hybridization. Like wild-type cells, HAATI^{STE}+Trt1 cells have rDNA only on Chr III (Fig. 2c). However, they have markedly amplified and rearranged STE sequences. Whereas wild-type chromosomes have STE sequences only on their terminal NotI restriction fragments, the STE probe hybridizes strongly with every NotI restriction fragment derived from HAATI^{STE} chromosomes, demonstrating that STE have spread to internal sites on Chr I and II (Fig. 2d). STE hybridization is also seen on Chr III of HAATI^{STE} cells (Supplementary Fig. 8b). Like all HAATI^{rDNA} chromosomes, all HAATI^{STE} chromosomes acquire telomeres and enter gels upon Trt1 reintroduction (Supplementary Fig. 8c). Dot blot analysis confirms the amplification of STE and rDNA sequences in HAATI^{STE} and HAATI^{rDNA}, respectively (Supplementary Table 2 and Supplementary Fig. 9).

Hence, although both classes of HAATI display DSB resistance, an inability of terminal chromosome fragments to enter gels, and

the acquisition of telomeres and chromosomal gel migration upon telomerase re-introduction, each has amplified a different class of repetitive sequence. In one case the rDNA has spread from the sub-terminal regions of Chr III to the termini of Chr I and II, whereas in the other case, STE sequences have spread from the terminal regions of Chr I and II to multiple sites in these chromosomes' interiors as well as onto Chr III. HAATI^{STE} survivors are exceedingly rare whereas HAATI^{rDNA} survivors are frequent (Supplementary Table 1), most likely reflecting the drastic genomic disruption that accompanies HAATI^{STE} formation. Therefore, the analyses below were performed on HAATI^{rDNA} except where indicated.

The rDNA and STE sequences of wild-type cells are packaged into heterochromatin characterized by histone H3-Lys9 (H3K9) hypermethylation^{16,17} and binding of Swi6, the fission yeast heterochromatin protein-1 (HP-1) orthologue. These hallmarks of the sequences amplified in HAATI raised the possibility that heterochromatin has a role in HAATI survival and indeed, the Swi6-green fluorescent protein (GFP) localization patterns of HAATI cells are consistent with expanded heterochromatin (Supplementary Fig. 10). Therefore, we investigated the requirement for the heterochromatin assembly machinery. Clr4, the single fission yeast orthologue of the Su(var.) 3-9 histone methyltransferase, is required for H3K9 methylation and heterochromatin formation¹⁸. *trt1Δclr4Δ* cells were isolated from heterozygous diploids and propagated under competitive conditions alongside *trt1Δ* single mutants. Whereas nearly all surviving *trt1Δ* cells exhibited HAATI survival (Supplementary Fig. 11a), most *trt1Δclr4Δ* cell populations comprised circular survivors (Fig. 3a and Supplementary Fig. 11b). Moreover, deletion of *clr4*⁺ in an already-formed haploid HAATI survivor led to immediate circularization of the chromosomes in 25% of cases (Fig. 3b), directly linking Clr4 to maintenance of HAATI. In contrast, Clr4 is dispensable for the maintenance of linear or circular *trt1Δ* survivors (Fig. 3b). As seen for *clr4*⁺, deletion of *swi6*⁺ severely compromises HAATI formation (Supplementary Fig. 12). The residual occurrence of HAATI in *clr4Δ* or *swi6Δ* cells lacking Trt1 may reflect heterochromatin function carried

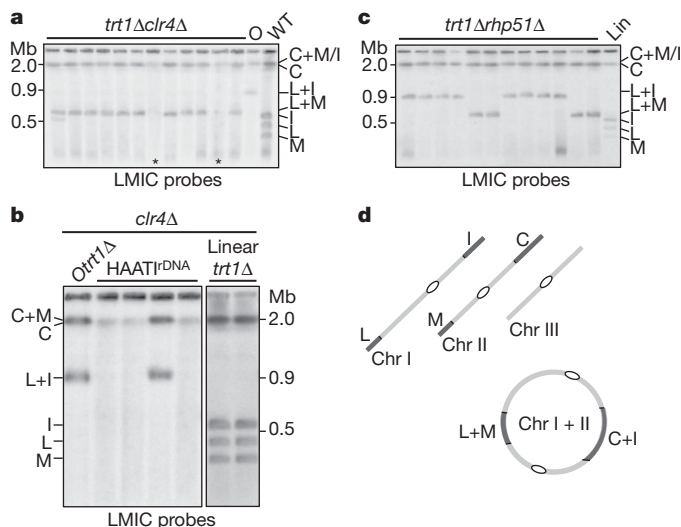


Figure 3 | HAATI survival requires Clr4 and Rhp51. **a**, Clr4 is important for HAATI formation. NotI digests of chromosomes of 12 *trt1Δclr4Δ* progeny derived from heterozygous *clr4Δ/clr4*⁺ *trt1Δ/trt1*⁺ diploids were grown in competitive conditions (see legend to Supplementary Table 1). Only 2/12 progeny (asterisks) gave HAATI-type hybridization patterns. **b**, Clr4 is important for HAATI maintenance. *clr4*⁺ was deleted in HAATI^{rDNA}, circular and linear *trt1Δ* strains. Clr4 is required for HAATI maintenance. To definitively assess a role for Clr4 in linear survival, 20 *clr4Δ* linear transformants were analysed (two are shown). None were affected by *clr4*⁺ deletion. **c**, HAATI survival requires Rhp51. *rhp51Δ/rhp51*⁺ *trt1Δ/trt1*⁺ diploids were treated as in **a**. 'Lin' denotes linear *trt1Δ*. **d**, Schematic of NotI fragments resulting from di-chromosome circle formation.

over from the parental strain, or a rare ability of cells to retain downstream heterochromatin functions (see later) following loss of these genes. Collectively, these results indicate that the heterochromatic nature of the sequences amplified in HAATI chromosomes is crucial to their formation and maintenance.

The repeat amplification seen in HAATI indicates that the relevant sequences sustain vigorous levels of recombination. Indeed, deletion of *rhp51*⁺ (which encodes the fission yeast Rad51 orthologue) abolishes HAATI formation, as all *trt1Δrhp51Δ* survivors raised in competitive conditions sustain circular chromosomes (Fig. 3b). Moreover, 9 out of 12 *trt1Δrad50Δ* survivors grown in competitive conditions form circular survivors (Supplementary Fig. 13). Hence, not only heterochromatin factors, but also Rhp51 and Rad50, are important for HAATI survival.

Curiously, the circular *trt1Δ* strains lacking Clr4, Swi6 or Rhp51 harbour di-chromosome circles (Fig. 3c and Supplementary Fig. 14). We speculate that dicentric circle formation reflects compromised centromere function in the absence of Clr4/Swi6 or Rhp51. Centromere inactivation, which would be necessary for propagation of dicentric chromosomes, may be frequent in the absence of Clr4/Swi6 or Rhp51 and may confer an advantage to dicentricity. Indeed, Clr4-based heterochromatin formation is a known requirement for centromere function¹⁹ and Rhp51 was shown to suppress rearrangement of centromeric sequences²⁰. Intriguingly, Rad50 does not seem to share a role in suppressing dicentric formation, as all *trt1Δrad50Δ* circulars isolated harbour mono-chromosomal circles (Supplementary Fig. 13).

The foregoing results suggest that HAATI chromosomes remain linear but fail to enter gels due to structures associated with the continual rearrangement of rDNA or STE sequences. The linearity of HAATI chromosomes made it crucial to ascertain whether they contain telomeric repeats; hence, we sought to release all terminal fragments for gel entry by digesting the genome with a cocktail of frequent-cutting restriction enzymes that do not digest telomere sequences. Digestion of wild-type or HAATI DNA with this cocktail reduces the majority of the genome to ≤ 100 bp fragments (Fig. 4a). Hybridization of digested wild-type DNA with a telomere probe reveals fragments of ~150–250 bp, as expected for the undigested telomeric repeat region. These fragments are sensitive to BAL-31 exonuclease treatment (Fig. 4b), confirming their localization to chromosomal termini. However, no telomeric hybridization is detected when cocktail-digested DNA from HAATI cells is probed at 65 °C, indicating that HAATI chromosomes lack stretches of telomeric DNA of greater than ~27 bp (see Methods). Hybridization at 55 °C, a temperature at which our probe should detect shorter telomere stretches, does yield a signal for DNA derived from HAATI^{rDNA} survivors (Fig. 4a). This signal runs as a discrete band, indicating localization to an internal rather than a terminal (and therefore heterogeneously sized) region. The size of this band corresponds to that expected for a region within the rDNA that contains a 13-bp stretch of telomeric sequence¹⁴, indicating that this signal arises as a by-product of the rDNA amplification in HAATI^{rDNA} survivors. Correspondingly, this short telomeric stretch resists extensive BAL-31 digestion (Fig. 4b), confirming its localization to the chromosomal interior rather than the terminus. No telomeric hybridization to HAATI^{STE} DNA was seen at 65 or 55 °C (Fig. 4a). Hence, HAATI^{rDNA} and HAATI^{STE} lack terminal telomeric repeat stretches.

The absence of telomere sequences at HAATI chromosome termini prompted us to investigate whether telomere proteins have a role in HAATI survival. Deletion of *taz1*⁺ has no effect on either HAATI subtype (Fig. 4c and Supplementary Fig. 15). Surprisingly, however, deletion of *pot1*⁺ from either HAATI^{STE} or HAATI^{rDNA} cells leads to chromosome circularization (Fig. 4c and Supplementary Fig. 15). Hence, chromosome end protection in HAATI cells requires Pot1 despite the absence of its canonical binding sites.

As the heterochromatin assembly machinery is required along with Pot1 for HAATI survival, our attention turned to Ccq1 as a

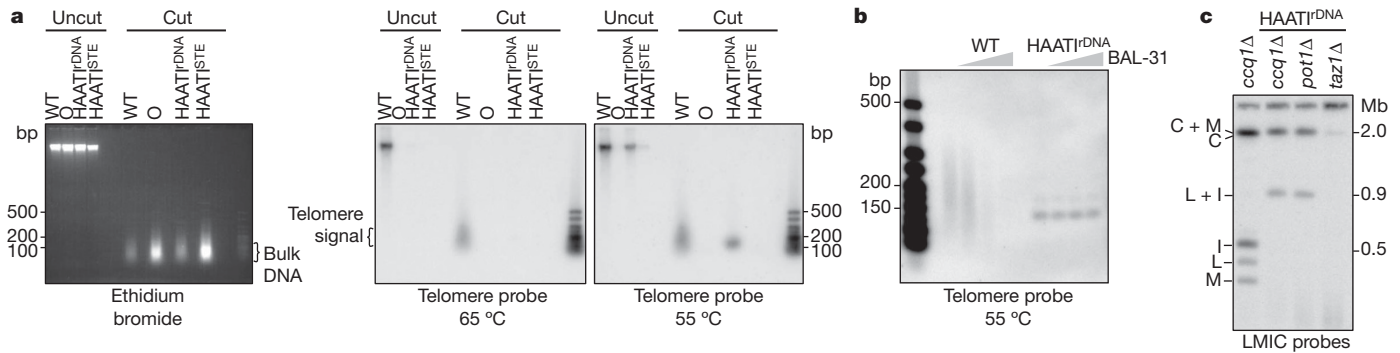


Figure 4 | HAATI strains lack terminal telomere sequences but require Pot1 for end-protection. **a**, HAATI^{STE} cells lack telomere sequences whereas HAATI^{rDNA} cells contain very short internal stretches of telomere-like sequence. Genomic DNA digested with restriction enzyme cocktail (see Methods) was subjected to Southern blotting. **b**, Telomere sequences in

potential Pot1 targeting factor. Ccq1 is a telomere-associated protein that forms a complex not only with Pot1, but also with the histone deacetylation machinery via the SHREC (Snf2/Hdac-containing repressor complex) heterochromatin complex^{5,21}. Thus, Ccq1 might serve as a link between the amplified heterochromatin and Pot1. Indeed, deletion of *ccq1*⁺ in HAATI^{rDNA} leads to immediate chromosome circularization (Fig. 4c). This result is particularly striking as *ccq1*⁺ deletion in wild-type cells promotes homologous recombination at telomeres, thereby opposing chromosome circularization²². Therefore, Ccq1 provides a chromosome end-protection function in HAATI cells that it does not provide in wild-type cells.

The foregoing data indicate that Pot1, which is required for preventing circularization of HAATI chromosomes, is recruited to HAATI chromosome ends by non-telomeric heterochromatin. As rDNA forms the termini of all HAATI^{rDNA} chromosomes, we propose that Pot1 localizes to these rDNA termini. Our attempts to detect rDNA in Pot1 immunoprecipitates were unsuccessful (Supplementary Fig. 16). This result is perhaps not unexpected given that the rDNA is amplified in HAATI^{rDNA} cells, giving rise to ~6 Mb of rDNA, of which only a vanishingly small fraction would constitute the Pot1 binding region if it is restricted to the rDNA terminus. This restriction to the terminus could be explained by a mechanism in which not only heterochromatin, but also a 3' overhang, contributes to Pot1 recruitment. Such a single-stranded overhang could bind Pot1 directly, in a non-sequence-specific manner, or indirectly via recruitment of ssDNA binding proteins like RPA, which may in turn interact with Pot1. Indeed, native in-gel hybridization analysis reveals an *Escherichia coli* ExoI-sensitive 3' single-stranded rDNA signal specifically in DNA from HAATI^{rDNA} strains; this rDNA overhang is abolished once bona fide telomeres have been added to the respective chromosome ends via Trt1 introduction (Supplementary Fig. 17). Hence, HAATI^{rDNA} chromosomes terminate with 3' overhangs of rDNA sequence.

Our data allow us to propose a model for the HAATI survival mode (Supplementary Fig. 1). The lack of high-affinity Pot1 binding sites (that is, telomeres) in HAATI cells enhances the availability of Pot1 for recruitment to non-telomeric heterochromatin by SHREC-Ccq1. Hence, the continual rearrangement and amplification of heterochromatic repeats insulates coding sequences from the end replication problem, while at the same time bringing Pot1 into the vicinity of the chromosome terminus. In addition, the presence of terminal 3' overhangs assists in concentrating Pot1 at the extreme chromosome end. Pot1 in turn provides an essential chromosome end-protection function. This function may be the restraint of 'runaway' 5' resection from the chromosomal terminus, as we have found that Pot1 inactivation leads to rampant telomeric C-strand loss²³. Inherent in this model is the idea that Pot1 serves an essential function without binding DNA directly, or by binding non-telomeric DNA sequences; we are currently probing which domains of Pot1 are essential for HAATI

survival and whether they are separable from those required for canonical telomere maintenance.

HAATI^{rDNA} cells are at internal genomic locations. Genomic DNA was treated with BAL-31 for 0, 15, 30 and 60 min and subsequently treated as in **a**. **c**, Analysis of NotI digests shows HAATI chromosome maintenance requires Pot1 and Ccq1, but not Taz1. A *ccq1*-deleted *trt1*⁺ strain is included for comparison.

The existence of HAATI shows that the telomere sequence per se is dispensable for chromosome linearity in fission yeast. Intriguing parallels can thus be drawn between HAATI survival and other instances in which 'generic' heterochromatin regulates chromosome dynamics in a manner usually associated with specific DNA sequences. Centromere identity is epigenetically determined in a number of organisms including fission yeast, in which centromere inactivation via excision of centromeric sequences can be bypassed by the assembly of kinetochores at subtelomeric sites^{24,25}. Moreover, the HAATI strategy for linear chromosome maintenance is reminiscent of the approach taken by *Drosophila* and other genera of Diptera^{26–28}. These organisms lack simple sequence repeats at their chromosomal termini, and although they often harbour terminal retrotransposons (HET or TART elements), the latter elements are dispensable for chromosome end maintenance. Crucially, regardless of the underlying sequences, *Drosophila* chromosome ends are packaged into heterochromatin, which is in turn associated with the recruitment of end-protection factors such as HOAP²⁹ and HipHop³⁰. Our data indicate that the exclusively epigenetic strategy may be more conserved than initially thought and may represent a universal solution to the problem of linear chromosome maintenance. The shared ability to use HAATI to maintain chromosome linearity in such widely divergent organisms as flies and yeast argues that such mechanisms may be possible in human cells as well. The rearrangements associated with HAATI could both promote tumorigenesis and provide a telomere-independent means by which cancer cells could attain unlimited proliferative capacity.

METHODS SUMMARY

All experiments were performed using the *Schizosaccharomyces pombe* strains, genetic manipulations and selection protocols described in Methods. Pulsed-field gel electrophoresis, hybridization analysis and restriction digest procedures are explained in Methods.

Full Methods and any associated references are available in the online version of the paper at www.nature.com/nature.

Received 7 September 2009; accepted 21 July 2010.

1. Palm, W. & de Lange, T. How shelterin protects mammalian telomeres. *Annu. Rev. Genet.* **42**, 301–334 (2008).
2. Rog, O. & Cooper, J. P. Telomeres in drag: dressing as DNA damage to engage telomerase. *Curr. Opin. Genet. Dev.* **18**, 212–220 (2008).
3. Blackburn, E. H. Telomeres and telomerase: their mechanisms of action and the effects of altering their functions. *FEBS Lett.* **579**, 859–862 (2005).
4. Baumann, P. & Cech, T. R. Pot1, the putative telomere end-binding protein in fission yeast and humans. *Science* **292**, 1171–1175 (2001).
5. Miyoshi, T., Kanoh, J., Saito, M. & Ishikawa, F. Fission yeast Pot1-Tpp1 protects telomeres and regulates telomere length. *Science* **320**, 1341–1344 (2008).

6. Dunham, M. A., Neumann, A. A., Fasching, C. L. & Reddel, R. R. Telomere maintenance by recombination in human cells. *Nature Genet.* **26**, 447–450 (2000).
7. Lundblad, V. & Blackburn, E. H. An alternative pathway for yeast telomere maintenance rescues *est1⁻* senescence. *Cell* **73**, 347–360 (1993).
8. Teng, S. C. & Zakian, V. A. Telomere-telomere recombination is an efficient bypass pathway for telomere maintenance in *Saccharomyces cerevisiae*. *Mol. Cell Biol.* **19**, 8083–8093 (1999).
9. McEachern, M. J. & Haber, J. E. Break-induced replication and recombinational telomere elongation in yeast. *Annu. Rev. Biochem.* **75**, 111–135 (2006).
10. Maringele, L. & Lydall, D. Telomerase- and recombination-independent immortalization of budding yeast. *Genes Dev.* **18**, 2663–2675 (2004).
11. Cooper, J. P., Nimmo, E. R., Allshire, R. C. & Cech, T. R. Regulation of telomere length and function by a Myb-domain protein in fission yeast. *Nature* **385**, 744–747 (1997).
12. Nakamura, T. M., Cooper, J. P. & Cech, T. R. Two modes of survival of fission yeast without telomerase. *Science* **282**, 493–496 (1998).
13. Wang, X. & Baumann, P. Chromosome fusions following telomere loss are mediated by single-strand annealing. *Mol. Cell* **31**, 463–473 (2008).
14. Sugawara, N. *DNA sequences at the telomeres of the fission yeast S. pombe*. PhD thesis, Harvard Univ. (1988).
15. Toda, T., Nakaseko, Y., Niwa, O. & Yanagida, M. Mapping of rRNA genes by integration of hybrid plasmids in *Schizosaccharomyces pombe*. *Curr. Genet.* **8**, 93–97 (1984).
16. Cam, H. P. *et al.* Comprehensive analysis of heterochromatin- and RNAi-mediated epigenetic control of the fission yeast genome. *Nature Genet.* **37**, 809–819 (2005).
17. Kano, J., Sadaie, M., Urano, T. & Ishikawa, F. Telomere binding protein Taz1 establishes Swi6 heterochromatin independently of RNAi at telomeres. *Curr. Biol.* **15**, 1808–1819 (2005).
18. Nakayama, J., Rice, J. C., Strahl, B. D., Allis, C. D. & Grewal, S. I. Role of histone H3 lysine 9 methylation in epigenetic control of heterochromatin assembly. *Science* **292**, 110–113 (2001).
19. Ekwall, K. *et al.* Mutations in the fission yeast silencing factors *clr4⁺* and *rik1⁺* disrupt the localisation of the chromo domain protein Swi6p and impair centromere function. *J. Cell Sci.* **109**, 2637–2648 (1996).
20. Nakamura, K. *et al.* Rad51 suppresses gross chromosomal rearrangement at centromere in *Schizosaccharomyces pombe*. *EMBO J.* **27**, 3036–3046 (2008).
21. Sugiyama, T. *et al.* SHREC, an effector complex for heterochromatic transcriptional silencing. *Cell* **128**, 491–504 (2007).
22. Tomita, K. & Cooper, J. P. Fission yeast Ccq1 is telomerase recruiter and local checkpoint controller. *Genes Dev.* **22**, 3461–3474 (2008).
23. Pitt, C. W. & Cooper, J. P. Pot1 inactivation leads to rampant telomere resection and loss in one cell cycle. *Nucleic Acids Res.* advance online publication, doi:10.1093/nar/gkq580 (3 July 2010).
24. Ishij, K. *et al.* Heterochromatin integrity affects chromosome reorganization after centromere dysfunction. *Science* **321**, 1088–1091 (2008).
25. Allshire, R. C. & Karpen, G. H. Epigenetic regulation of centromeric chromatin: old dogs, new tricks? *Nature Rev. Genet.* **9**, 923–937 (2008).
26. Mason, J. M., Frydrychova, R. C. & Biessmann, H. *Drosophila* telomeres: an exception providing new insights. *Bioessays* **30**, 25–37 (2008).
27. Cenci, G., Ciapponi, L. & Gatti, M. The mechanism of telomere protection: a comparison between *Drosophila* and humans. *Chromosoma* **114**, 135–145 (2005).
28. Pardue, M. L. & DeBaryshe, P. G. Retrotransposons provide an evolutionarily robust non-telomerase mechanism to maintain telomeres. *Annu. Rev. Genet.* **37**, 485–511 (2003).
29. Cenci, G., Siriaco, G., Raffa, G. D., Kellum, R. & Gatti, M. The *Drosophila* HOAP protein is required for telomere capping. *Nature Cell Biol.* **5**, 82–84 (2003).
30. Gao, G. *et al.* HipHop interacts with HOAP and HP1 to protect *Drosophila* telomeres in a sequence-independent manner. *EMBO J.* **29**, 819–829 (2010).

Supplementary Information is linked to the online version of the paper at www.nature.com/nature.

Acknowledgements We thank T. Cech for discussions and gratefully acknowledge that initial work by T.M.N. on reintroducing Trt1 to circular strains was performed in the Cech laboratory. We thank our current and former laboratory members for discussions and advice. This work was supported by Cancer Research UK.

Author Contributions D.J. performed the experiments in Figs 3 and 4, Supplementary Figs 6 and 9–17 and Supplementary Tables 1 and 2, and reproduced Figs 1a, b, 2a, d and Supplementary Figs 2 and 8a. A.K.H. first isolated HAATI survivors and performed the experiments in Figs 1 and 2b–d, and Supplementary Figs 2, 4, 5 and 8. T.M.N. performed the experiments in Fig. 2a. K.M.M. first showed that circular strains are hypersensitive to DSB-inducing agents. J.P.C. designed and supervised the study. J.P.C. and D.J. generated the figures and wrote the paper.

Author Information Reprints and permissions information is available at www.nature.com/reprints. The authors declare no competing financial interests. Readers are welcome to comment on the online version of this article at www.nature.com/nature. Correspondence and requests for materials should be addressed to J.P.C. (julie.cooper@cancer.org.uk).

METHODS

Strains and media. Strains used in this study are listed in Supplementary Information.

trt1Δ/trt1⁺, *clr4Δ/clr4⁺* *trt1Δ/trt1⁺*, *rhp51Δ/rhp51⁺* *trt1Δ/trt1⁺*, *swi6Δ/swi6⁺* *trt1Δ/trt1⁺* and *rad50Δ/rad50⁺* *trt1Δ/trt1⁺* strains were made by one-step gene replacement in wild-type diploids.

taz1Δ HAATI^{rDNA}, *taz1Δ* HAATI^{STE}, *pot1Δ* HAATI^{rDNA}, *pot1Δ* HAATI^{STE}, *ccq1Δ* HAATI^{rDNA}, *clr4Δ* HAATI^{rDNA}, *clr4Δ* circular *trt1Δ* survivor and *clr4Δ* linear *trt1Δ* survivor strains were constructed by one-step gene replacement in already-formed HAATI survivors, already-formed circular survivors and already-formed linear survivors, respectively. GFP, red fluorescence protein (RFP) and 6PK tags were integrated at the endogenous C termini of *swi6⁺*, *hht1⁺* and *pot1⁺* by one-step gene replacement in wild type or already-formed circular or HAATI survivor strains.

Strains containing the I-SceI restriction site were constructed by inserting the I-SceI recognition sequence along with a KanMX cassette downstream of the *his4* locus by one-step gene replacement in wild type, already-formed circular and already-formed HAATI survivors. The presence of the site was verified by Southern analysis.

Strain 956 had an internal telomere at *ura4* for use in experiments not described in this manuscript. Strain 8500 was derived from 956 by deletion of the internal telomere at *ura4*. None of the other strains contain this internal telomere stretch. ‘+ Trt1’ strains were constructed by transforming p-kanMX-*trt1⁺*-myc (ref. 31) into the indicated strains.

Strains were grown at 32 °C in standard rich media (yeast extract media with supplements (YES), or yeast extract media with low adenine concentration (YE) for diploids)³².

Cytological analysis. Cells were grown to log phase in rich media at 32 °C and visualized by light and fluorescence microscopy.

To visualize nuclear morphology, cells were fixed in 70% ethanol, rehydrated in water, stained with DAPI (Vector Laboratories) and imaged on a Zeiss Axioplan 2 microscope (Carl Zeiss MicroImaging) with an attached CCD camera (Hamamatsu). Images were captured and analysed using Velocity software (Improvision).

Swi6-GFP and Hht1-RFP were visualized as described previously³³, with the following modifications: cells adhered to glass culture dishes were immersed in Edinburgh minimal media with required supplements. Images were captured with equal exposure for all cell types and images presented here are representative of 17 nuclei. Images were deconvolved and all Z-stacks projected into a single image.

Pulsed-field gel electrophoresis of whole chromosomes. PFGE of whole chromosomes was performed as described previously³⁴, with the following modifications: cells were spheroplasted with 0.6 mg ml⁻¹ Zymolase-100T (Immuno) at 37 °C for 30 to 45 min, resuspended in 1% low melting point agarose (Invitrogen) at a concentration of 10⁸ cells per 100 μl. Agarose plugs were loaded onto 0.8% agarose gels. PFGE was performed on a BioRad CHEF DR-III system in 1× TAE (40 mM Tris-acetate buffer, 2 mM Na₂EDTA (pH 8.3)) at 14 °C using the following program: step 1, 24 h at 2 V cm⁻¹, 96° angle, 1,200 s switch time; step 2, 24 h at 2 V cm⁻¹, 100° angle, 1,500 s switch time; 24 h at 2 V cm⁻¹, 106° angle, 1,800 s switch time. Gels for Figs 1b and 2a and Supplementary Fig. 6 were 0.5% agarose, run 30 h for each step. After electrophoresis, DNA was visualized by ethidium bromide staining, and gels were processed for Southern blotting, which was performed using a telomeric probe³⁵, the STE1 probe (from pNSU70 as described previously¹²), the rDNA probe¹⁶ or PCR products of *cdc3* gene (used as a probe to visualize Chr I) or the *his4* gene (used as a probe to visualize Chr II).

For analysis of chromosomal cleavage by γ radiation, plugs containing the indicated strains were exposed to the indicated doses as described previously³⁶ and processed for PFGE as described above.

PFGE of restriction-enzyme-digested chromosomes. For I-SceI restriction digests, agarose plugs were preincubated at 4 °C in 0.1 M diethanolamine (pH 9.5) overnight. Each plug was then preincubated on ice in 160 μl 0.1 M diethanolamine (pH 9.5), 0.001 M dithiothreitol and 0.02 mg ml⁻¹ BSA for 1 h. ‘Enhancer’ (Roche, 2 μl) was added along with 30–40 units I-SceI (Roche) and allowed to diffuse into the plugs on ice for 2 h. MgCl₂ was added to a final concentration of 8 mM to activate the enzyme and plugs were incubated at 37 °C for 1 h. PFGE was performed as described above.

For NotI restriction digest, plugs were pre-equilibrated in 2× NotI buffer (NEBuffer 3) and 20 μg ml⁻¹ BSA for 1 h before digestion. Buffer was replaced with 1× NotI buffer, 10 μg ml⁻¹ BSA and 100 units of NotI and incubated overnight at 37 °C. NotI-digested agarose plugs were loaded onto 1% agarose gels in 0.5× TBE (1× TBE: 89 mM Tris-borate and 2 mM EDTA). PFGE was performed on a Bio-Rad CHEF DR-III system in 0.5× TBE at 14 °C using the following program: 24 h at 6 V cm⁻¹, 120° angle, 60–120 s switch time. DNA was visualized by ethidium bromide staining and gels were subjected to Southern

blot analysis using LMIC probes³⁴, the STE1 probe (from pNSU70 as described previously¹²) or the rDNA probe¹⁶.

Restriction enzyme cocktail digestion. Genomic DNA was digested with Hpy188III, DdeI, DpnI, HincII, AluI, MseI and AclI in 1× NEBuffer 2 and 10 μg ml⁻¹ BSA at 37 °C overnight. DNA was then ethanol-precipitated, run on a 2% agarose gel and subjected to Southern blot analysis. To detect telomeres, a random-prime labelled synthetic telomeric oligonucleotide probe (described in ref. 35) was used. Briefly, this 450-bp probe comprises ligated annealed oligonucleotides of 49 bp of telomeric sequence. Hybridization was performed at either 65 °C or 55 °C. As predicted by ApE (Aplasmid Editor v1.14), 55 °C corresponds to the *T_m* for hybridization of this probe to a ~19-bp region of homology and 65 °C corresponds to the *T_m* for hybridization to a ~27-bp region. However, the substantial degeneracy of fission yeast telomere sequences¹⁴ prohibit the derivation of precise predictions for hybridization efficiency.

Nuclease BAL-31 digestion. Genomic DNA was incubated with linear plasmid DNA (as control) and 20 units of BAL-31 in 1× BAL-31 buffer (NEB) for the indicated times at 30 °C. Reactions were heat-inactivated at 65 °C in the presence of 20 mM EGTA. DNA was phenol-chloroform-extracted, ethanol-precipitated and an aliquot run on a 1% agarose gel to assess digestion via a decrease in size of the linear plasmid. Digested samples were then subjected to restriction enzyme cocktail digestion and Southern blot analysis as described above.

In-gel hybridization. Genomic DNA was digested with HindIII in NEBuffer 2 at 37 °C overnight. In-gel hybridization was performed as previously described³⁷. The HindIII fragment of YIp10.4 used as the rDNA probe¹⁶, either in its native condition or alkaline denatured, was used as control.

Nuclease ExoI digestion. Genomic DNA was incubated with 40 units of ExoI in 1× ExoI buffer (NEB) overnight at 37 °C. DNA was phenol-chloroform-extracted and ethanol-precipitated. Treated samples were subjected to restriction enzyme digestion and in-gel hybridization as described above.

Chromatin immunoprecipitation. Log-phase cultures (50 ml) of indicated strains were incubated for 15 min at 25 °C with 1% formaldehyde to crosslink chromatin. Cells were then pelleted and washed twice in cold PBSA. The pellet was resuspended in 500 μl lysis buffer (50 mM HEPES (pH 7.5), 140 mM NaCl, 1 mM EDTA, 1% IGEPAL CA-630, 0.1% sodium deoxycholate, 1 mM PMSF, 100 μg μl⁻¹ protease inhibitor MG132 (Sigma), 1× Protease Inhibitors Cocktail Set III (Calbiochem, 1,000×)) and equal volume of glass beads. Cells were broken using a Fast Prep machine (Thermo). The lysate was recovered and centrifuged for 30 min. The top-most clear layer was discarded and the middle layer (crosslinked chromatin) along with the pellet was resuspended in lysis buffer. The samples were sonicated with a BIORUPTOR (Diagenode). Samples were centrifuged and supernatant recovered, an aliquot kept as whole-cell extract (WCE) and the rest used for immunoprecipitation. Mouse anti-V5 tag antibody (Serotec) that had been incubated with pan mouse IgG-coated magnetic Dynabeads (Invitrogen) overnight was incubated with lysate samples for 2 h. Beads were pulled down using a magnet, washed twice in SDS buffer (50 mM HEPES, 1 mM EDTA, 140 mM NaCl, 0.025% SDS), once in high salt buffer (50 mM HEPES, 1 mM EDTA, 0.5 M NaCl), once in T/L solution (20 mM Tris-Cl (pH 7.5), 10.7 mg ml⁻¹ LiCl, 1 mM EDTA, 150 μl IGEPAL-CA630, 0.15 g NaDOC), twice in T/E solution (20 mM Tris-Cl (pH 7.5), 0.1 mM EDTA), resuspended in TE + 1% SDS and heated at 65 °C for 15 min. The beads were pulled down using a magnet and supernatant recovered. IP and WCE were reverse cross-linked at 65 °C for 16 h, incubated with RNase A at 37 °C for 1 h, then concentrated using a Qiagen QIAquick PCR Purification kit. The eluted DNA was transferred to a 96-well microtitre plate. WCE samples were serially diluted five-fold in TE. DNA was processed for Southern blotting as described below. The probes used were rDNA probe¹⁶ and telomeric probe³⁵.

Dot blot analysis. Genomic DNA (Supplementary Fig. 9) or DNA obtained from reverse crosslinked WCE and immunoprecipitation (Supplementary Fig. 16), diluted as indicated, was added to 96-well microtitre plates and incubated with 10 ml of denaturation buffer (60 mg ml⁻¹ NaOH, 3.125 M NaCl) for 10 min. Dilution buffer (130 ml; 0.1× SSC, 0.125 M NaCl) was added for 5 min on ice. The DNA was vacuum-spotted using the S&S Minifold I Dot-Blot System (Schleicher & Schuell) onto a membrane pre-equilibrated with dilution buffer. The membrane was crosslinked, washed in neutralization buffer (0.5 M Tris-Cl (pH 7.5), 0.5 M NaCl) and then probed as indicated. The signals were visualized using a STORM 860 PhosphorImager Scanner (Molecular Dynamics) and quantified using ImageQuant TL (GE Healthcare). The probes used were: a PCR product for *act1* gene to normalize for DNA quantity, rDNA probe¹⁶ and STE1 probe (from pNSU70 as described previously¹²).

31. Haering, C. H., Nakamura, T. M., Baumann, P. & Cech, T. R. Analysis of telomerase catalytic subunit mutants *in vivo* and *in vitro* in *Schizosaccharomyces pombe*. *Proc. Natl Acad. Sci. USA* **97**, 6367–6372 (2000).

32. Moreno, S., Klar, A. & Nurse, P. Molecular genetic analysis of fission yeast *Schizosaccharomyces pombe*. *Methods Enzymol.* **194**, 795–823 (1991).

33. Tomita, K. & Cooper, J. P. The telomere bouquet controls the meiotic spindle. *Cell* **130**, 113–126 (2007).
34. Ferreira, M. G. & Cooper, J. P. The fission yeast Taz1 protein protects chromosomes from Ku-dependent end-to-end fusions. *Mol. Cell* **7**, 55–63 (2001).
35. Miller, K. M., Rog, O. & Cooper, J. P. Semi-conservative DNA replication through telomeres requires Taz1. *Nature* **440**, 824–828 (2006).
36. Ferreira, M. G. & Cooper, J. P. Two modes of DNA double-strand break repair are reciprocally regulated through the fission yeast cell cycle. *Genes Dev.* **18**, 2249–2254 (2004).
37. Tomita, K. *et al.* Competition between the Rad50 complex and the Ku heterodimer reveals a role for Exo1 in processing double-strand breaks but not telomeres. *Mol. Cell. Biol.* **23**, 5186–5197 (2003).